Unveiling kaempferol glycosides as the key antiglycative components in butterfly pea (*Clitoria ternatea*) flower

Jun Wu [a,b], Jun Gong [c], Qiaochun Chen [a], Wen Hao [d,e], Jiayi He [b], Mingfu Wang [b,*], Qian Zhou [f,g,**]

[a] *Institute for Advanced Study, Shenzhen University, Shenzhen, 518060, China*
[b] *Shenzhen Key Laboratory of Food Nutrition and Health, College of Chemistry and Environmental Engineering, Shenzhen University, Shenzhen, 518060, China*
[c] *Central Laboratory of YunFu People's Hospital, Yunfu, 527300, China*
[d] *Qingdao Municipal Center for Disease Control and Prevention, Qingdao, 266000, China*
[e] *Qingdao Institute of Preventive Medicine, Qingdao, 266000, China*
[f] *State Key Laboratory of Food Science and Resources, Jiangnan University, Wuxi, 214122, China*
[g] *School of Food Science and Technology, Jiangnan University, Wuxi, 214122, China*

ARTICLE INFO

ABSTRACT

Edible flowers have been used in dietary practices since ancient times. In recent years, they have garnered increasingly more attentions for their potentials in the prevention and amelioration of pathological conditions. The present study employed *in vitro* BSA models to evaluate the antiglycative effect of some edible flowers. Results showed that butterfly pea flower (BFPF) exhibited the highest potential in preventing advanced glycation end products (AGEs) formation, which had an inhibition rate of 92.11% at 1 g/mL, 56.99% at 0.1 g/mL, and 9.94% at 0.01 g/mL, respectively. Moreover, the antiglycative components in BFPF were identified as four flavonol glycosides through chromatographic and spectral analyses, which were manghaslin (quercetin 3-2″-rhamnosylrutinoside, QCT-Rh), clitorin (kaempferol 3–2″-rhamnosylrutinoside, KFR-Rh), rutin (quercetin 3-rutinoside), and kaempferol 3-neohesperidoside (KFR-Ne). Notably, KFR-Rh and KFR-Ne were presented in higher concentrations in BFPF (764.31 mg/kg and 1135.10 mg/kg dry matter) and significantly contributed to the antiglycative activity (IC_{50} = 182.17 μM and IC_{50} = 131.03 μM). Molecular docking (MD) and nuclear magnetic resonance (NMR) analyses revealed that KFR-Rh and KFR-Ne formed hydrogen bonds and hydrophobic interactions with BSA, while KFR-Ne demonstrating a stronger interaction than KFR-Rh. Collectively, our findings highlight the beneficial effects of BFPF with clearly identified active components, which might further promote its application in functional food and medical industry.

1. Introduction

Edible flowers have been historically consumed in dishes such as salads and soups with the purpose of enhancing flavor, taste and/or visual appeal in European and Asian countries (Chen et al., 2020). They also serve as spices and natural colorants in bakeries, desserts, and beverages, augmenting aesthetic and gustatory qualities. Moreover, edible flowers hold appreciable health benefits against obesity, cardiovascular diseases, hepatic dysfunctions, and cancer (Rivas García et al., 2021). For instance, flowering rosemary (*Rosmarinus officinalis* L.) inhibited the proliferation and survival of prostate cancer cell by

targeting Protein Kinase B (Akt) and Mammalian Target of Rapamycin (mTOR) signaling pathways (Jaglanian et al., 2020). The flowers of dandelion (*Taraxacum officinale* L.) exhibited anti-cancer activity by triggering G2/M phase arrest and inhibiting cell apoptosis in MDA-MB-231 cells (Li et al., 2017). Rose (*Rosa rugosa*) demonstrated an appreciable hepatoprotective effect on alcohol-induced apoptosis through the activation of Sirtuin1 (SIRT1)/Adenosine Monophosphate-activated Protein Kinase (AMPK) signaling pathway (Zhou et al., 2021). Such beneficial effects make edible flowers a promising material/ingredient in the developing of functional foods. Additionally, edible flowers can be recognized as cash crops to some

extent, facilitating the economic development of flower-producing countries and places through the identification of a new niche market. Therefore, the study of edible flowers has gradually received increasingly more interests over years.

Among all edible flowers, butterfly pea (*Clitoria ternatea*) flower (BFPF) has particularly attracted our attentions, primarily owing to their diverse applications in bakeries, coffees, and sweetened beverages. Butterfly pea, belonging to the Fabaceae family, is widely cultivated in tropical and temperate regions. And its flower is commonly utilized as natural colorant in various foods and beverages, as well as being an indicator for food freshness more recently (Hashim et al., 2022; Jeyaraj et al., 2021). This is mainly attributed to its abundance of acylated anthocyanins in BFPF, which exert a distinguished and stable blue color (Escher et al., 2020). Moreover, numerous studies have exemplified their appreciable anti-inflammatory, antioxidant, and anti-cancer activities (López Prado et al., 2019; Nair et al., 2015; Shen et al., 2016). For example, BFPF ameliorated lipopolysaccharide (LPS)-induced inflammatory responses through suppressing Toll-like Receptor (TLR) dependent pathway (Nair et al., 2015). BFPF can also effectively prevent hyperglycemia, enhance blood lipid profiles, restore immune balance between regulatory T (Treg)/T helper 17 (Th17) cells, and inhibit liver and abdominal white adipose tissue accumulation (Yu et al., 2023). These beneficial effects were possibly due to the existence of polyphenols, in particular, quercetin glycosides (e.g., rutinoside, rhamnosylrutinoside, and neohesperidoside) and anthocyanidins (e.g., ternatin A1-A3, B1-B4, C1-C5, and D1-D3) (Kazuma, Noda and Suzuki, 2003a, 2003b).

During our previous work, we found some edible flowers exhibited potentials in preventing the formation of advanced glycation end products (AGEs) (Jiayang Gao, Sun, Li, Zhou and Wang, 2020). AGEs play a crucial role in the occurrence and development of vascular complications associated with diabetes. It has been firmly established that inhibiting AGEs formation acts as a means to combat the deleterious effects of hyperglycemia, thereby preventing and ameliorating diabetes and its associated complications (Zhou et al., 2020). Intriguingly, a plethora of recent studies have also illustrated the role of glycation in the aging process (Wen et al., 2022). AGEs might be an aging biomarker as their amount increased in physiological (e.g. skin, eyes, and joints) and pathological (e.g. neurodegenerative and cardiovascular diseases) aging structures (H. Peng et al., 2024). Except being a biomarker, AGEs act as a potential driver of aging process since a linear increase in the amounts of glycated products was observed with age. Furthermore, AGEs can bind to the receptor for AGEs (RAGE), initiating a signaling cascade to induce oxidative and inflammatory status through activating nuclear factor-κB (NF-κB). On the other hand, the accumulation of oxidative stress and inflammation accelerates the aging process (Chaudhuri et al., 2018). Some precursors of AGEs can also crosslink with proteins such as collagen which leads to skin loss of elasticity, and capture low-density lipoprotein molecules which are related with arterial diseases and showed significance in aging studies (Yue et al., 2023). Thus, it is crucial to prevent the formation of AGEs, which might be an effective strategy to ameliorate AGEs-associated diabetic complications and delay aging process. However, although there is a wide range of edible flowers existed, the research on evaluating their antiglycative potential and identifying the responsible compounds is still incomplete.

Considering the functional benefits of edible flowers, the present study aimed to expand the scope of edible flowers that were able to inhibit the formation of AGEs and to offer practical advice for consumers who pursue anti-aging foods. The flowers included BFPF, Sophora (*Sophora japonica* (L.)) flower, dandelion (*Taraxacum mongolicum* (Hand.-Mazz.)) flower, safflower (*Carthamus tinctorius* (L.)), pumpkin (*Cucurbita moschata* (Duch. ex Lam.) Duch. ex Poiret) flower, coffee (*Coffea arabica* (L.)) flower, peanut (*Arachis hypogaea* (L.)) flower, and artichoke (*Cynara scolymus* (L.)) flower. The most antiglycative one was chosen for further investigation, with its main active compounds identified through chromatographic and spectral analyses. Subsequently, the action

mechanism of the identified antiglycative compounds was evaluated by molecular docking (MD) and nuclear magnetic resonance (NMR) analyses.

2. Material and methods

2.1. Chemicals and reagents

Edible flowers were purchased from Yufeng (Taizhou, Jiangsu, China). Ethanol, methanol, fructose, petroleum ether, n-hexane, ethyl acetate, dichloromethane, acetone, formic acid, and deuterium hydrogen oxide were bought from Macklin (Shanghai, China). Phosphate buffered saline (PBS) was bought from Beyotime Biotech (Shanghai, China). Bovine serum albumin (BSA), d-glucose, and HPLC grade acetonitrile (ACN) were bought from Sigma-Aldrich (St. Louis, MO, USA), while LC-MS grade ACN was from Thermo Fisher (Waltham, MA, USA). All of the standard chemicals were products of ChemFaces (Hubei, China), which including kaempferol (KFR), clitorin (kaempferol 3–2″-rhamnosylrutinoside, KFR-Rh), kaempferol 3-neohesperidoside (KFR-Ne), manghaslin (quercetin 3-2″-rhamnosylrutinoside, QCT-Rh), and rutin (quercetin 3-rutinoside).

2.2. Preparation of flower extracts

Ten grams of each dried flower were ground into powders, added with 100 mL of 95% ethanol, ultrasonically extracted with an ultrasonic apparatus (Shumei, Kunshan Ultrasonic Instrument co. ltd., Kunshan, China) at the frequency of 40 kHz for 30 min at room temperature, and filtered through filter paper (Jiaojie, Fushun, China). The filtrate was collected, while the residue was ultrasonically extracted with 100 mL of ethanol for another two times. All of the filtrates were combined, vacuum evaporated to dryness under 40 °C using a rotary evaporator (EYELA, Tokyo, Japan), and then re-dissolved in 10 mL methanol. All extracts were stored at −20 °C until use.

2.3. Antiglycative activity screening of flower extracts in BSA models

To compare the antiglycative capability of these flower extracts, fructose-BSA (Fru-BSA) and glucose-BSA (Glu-BSA) models were set up, according to previous study (Jiayang Gao et al., 2020). Briefly, 45.05 g fructose or glucose was added with 5 g BSA in 100 mL PBS to get a final concentration of 2.5 M sugar and 50 mg/mL BSA solution. For each BSA model, 1 mL prepared solution was mixed with 50 μL of each flower extract (undiluted, 10-fold, and 100-fold diluted, separately) as experimental groups, whilst 1 mL of prepared solution was mixed with 50 μL methanol as the control group. After that, all solutions were incubated at 37 °C for 7 days, and then 200 μL of each solution was transferred into a black 96-well plate (SPL LIFE SCIENCES, Gyeonggi-do, Korea). The fluorescent intensity of formed AGEs was measured with excitation/emission wavelength at 370/440 nm using a fluorescent microplate reader (BioTek, Winooski, USA). The AGEs inhibition rate of each flower extract was calculated by the following equation:

$$AGEs\ inhibition\ rate\ (\%) = \left(1 - \frac{Trt}{Ctl}\right) \times 100$$

Trt: fluorescent intensity of flower extract; Ctl: fluorescent intensity of control solution.

2.4. Fractionation of butterfly pea flower extract for antiglycative components

Twenty grams of butterfly pea flower was ground into powder, ultrasonically extracted with 200 mL petroleum ether for 30 min at room temperature and filtered. The filtrate was collected, while the residue was ultrasonically extracted with 200 mL n-hexane, ethyl acetate, 95%

ethanol, and distilled water in sequence using the same extraction process. The antiglycative activity of these five extracts was detected using Fru-BSA model mentioned in section 2.3. Following that, the extract with the highest AGEs inhibitory rate was vacuum evaporated, followed by open column fractionation according to a previous study (Zhou et al., 2021). To be specific, the residue was loaded onto a silica gel column (60 mm × 50 cm) and successively eluted with 500 mL n-hexane, 500 mL n-hexane and ethyl acetate mixture (4:1 and 1:4), 500 mL ethyl acetate, 250 mL dichloromethane and methanol mixture (4:1, 1:1, and 1:4), and 500 mL methanol. 16 fractions were collected, labelled as A1 to A16, and their antiglycative activity was evaluated using Fru-BSA model. The most effective fraction was again evaporated to dryness, loaded onto a second silica gel column (30 mm × 35 cm) and eluted by 200 mL n-hexane, 200 mL dichloromethane and methanol mixture (4:1, 1:4, and 1:8). Subsequently, the most effective fractions were combined and evaporated, re-dissolved, loaded onto a Sephadex LH-20 column (30 mm × 35 cm), and eluted with 500 mL methanol. 13 eluates were collected, marked as C1 to C13, and their antiglycative activity was evaluated.

2.5. Identification of the antiglycative compounds in butterfly pea flower

After the final column fractionation, the most effective fraction was analyzed via HPLC and LC-MS analyses. HPLC was performed in Waters Arc HPLC System with a 2998 photodiode array detector (Waters corporation, Milford, MA, USA) and a XBridge C_{18} column (4.6 mm × 250 mm, 5 μm particle size, Waters, Milford, MA). The injection volume was 10 μL. The mobile phase was 0.1% formic acid and ACN, with gradient elution from 10% to 85% in 45 min and a flow rate of 1 mL/min. The wavelength scan was from 200 to 400 nm. LC-MS analysis was performed using a Waters ACQUITY UPLC H-Class chromatographic system (Waters, Milford, MA) coupled with a XEVO TQ-XS tandem triple quadrupole mass spectrometer (Waters, Milford, MA). A Waters ACQUITY UPLC BEH C_{18} column (2.1 mm × 100 mm, 1.7 μm) was empolyed, with column temperature set at 35 °C. The mobile phase was 0.1% formic acid and ACN. The gradient elution was 5%–90% within 35 min at a flow rate of 0.2 mL/min. The injection volume was 3 μL. Additionally, the ESI-MS operating conditions were set as follows: ionization mode, positive (ESI+) and negative (ESI-); ion source temperature, 120 °C; desolvation temperature, 500 °C; capillary voltage, 2.5 kV; cone gas flow rate, 150 L/h; desolvation gas flow rate, 1000 L/h, collision gas flow rate, 0.15 mL/min. The full MS scan was from 50 to 1500 m/z. The extracted ion chromatogram (XIC) of a specific m/z and their product ion spectra were recorded.

2.6. Molecular docking of the antiglycative compounds in butterfly pea flower

AutoDock 4.2.6 software (https://autodock.scripps.edu/) with the AutoDockTools 1.5.6 was employed for docking studies. Site specific BSA were docked with fructose, KFR, KFR-Rh, and KFR-Ne. The following parameters were adopted: grid maps 379,566 points, grid-point spacing 0.375 Å, number of genetic algorithms 10. PyMOL 2.2.0 software (The PyMOL Molecular Graphics System, Schrödinger, LLC.) and Protein-Ligand Interaction Profiler website (https://plip-tool.biotec.tu-dresden.de/plip-web/plip/index) was used to generate high-resolution figures to present the crystal structures.

2.7. NMR analysis of BSA and kaempferol glycosides

NMR analysis was performed to verify the interaction between BSA and KFR glycosides, following the method described by Zhang et al. with minor modifications (Chuan ying et al., 2021). In brief, KRF-Ne or KFR-Rh was mixed with BSA at the ratio of 100:1. The final concentration of KFR-Ne and KFR-Rh was kept as 2.5 mM, with D_2O as the solvent. Meanwhile, 2.5 mM pure KFR-Ne and KFR-Rh were used as

reference data. All solutions were incubated at 37 °C for 7 days. Subsequently, ^1H NMR spectral data were recorded at 400 MHz in a superconducting NMR spectrometer (Bruker Avance NEO 400, MA, USA).

2.8. Statistical analysis

The results were expressed as mean ± standard deviation (SD), derived from at least three independent replicates. Each replicate included separate experimental trials conducted under controlled conditions to ensure result reliability. Group means were compared using one-way analysis of variance (ANOVA), followed by Tukey's test for multiple comparisons. Statistical significance was determined at p < 0.05. Data analyses and figure generation were carried out using GraphPad Prism 9.0 (GraphPad Software Inc., San Jose, CA, USA), Origin 2021 (OriginLab Corporation, Northampton, MA, USA), and MestReNova 14.0 (Mestrelab Research, Santiago de Compostela, Spain).

3. Results and discussion

3.1. Antiglycative activity of various edible flowers

In the present study, fructose and glucose were individually utilized to create a hyperglycemia environment and simulate reactions with BSA. As shown in Fig. 1A, the AGEs inhibition rate of 1 g/mL samples were as follows: BFPF (92.11 ± 0.20%) > sophora (89.40 ± 0.42%) > dandelion flower (83.59 ± 0.76%) > safflower (80.15 ± 1.30%) > pumpkin flower (67.80 ± 1.16%) > coffee flower (62.13 ± 0.75%) > peanut flower (28.96 ± 4.56%) > artichoke (21.84 ± 1.13%) in Fru-BSA model. Since the results of some flowers were very close, we further explored their inhibition rates at 0.1 g/mL flower in methanol (Figs. 1B) and 0.01 g/mL flower in methanol (Fig. 1C). In the 0.1 g/mL samples, the inhibition order was as BFPF (56.99 ± 0.61%) > sophora (50.60 ± 1.26%) > dandelion flower (50.41 ± 1.71%) > coffee flower (35.35 ± 0.85%) > safflower (30.55 ± 1.18%) > pumpkin flower (26.79 ± 0.31%) > peanut flower (17.60 ± 1.43%) > artichoke (16.53 ± 0.27%). However, all eight flowers demonstrated poor anti-glycative effects (ranging from 1.62 ± 0.27% to 14.63 ± 0.21%) at 0.01 g/mL level, with minimal differences in their efficacy. In the Glu-BSA model, BFPF maintained their superior antiglycative effect and the observed trends in efficacy among the flower extracts were similar to the Fru-BSA model (Fig. 1E–G). In particular, the data in the 1 g/mL was BFPF (90.13 ± 0.26%) > sophora (87.41 ± 0.80%) > dandelion flower (81.09 ± 1.35%) > safflower (74.68 ± 1.28%) > pumpkin flower (62.26 ± 2.47%) > coffee flower (51.48 ± 1.17%) > artichoke (15.29 ± 2.79%) > peanut flower (8.17 ± 4.32%). Notably, the activity of fructose in the formation of Maillard reaction products was reported to be 8–10 times higher than that of glucose (Gugliucci, 2017). But in our study, the fluorescent intensity in the Fru-BSA system was 1.23 times higher than glucose. Another thing is that we noticed a lower antiglycative effect of the flowers in the Glu-BSA model compared to the Fru-BSA model, potentially attributed to the increased stability of the open-chain form and keto group of fructose (Gugliucci, 2017). Additionally, atypical rates were observed in peanut flower. The 1 g/mL concentration (8.17 ± 4.32%) antiglycative effect of peanut flower in the Glu-BSA was lower than that of artichoke (15.29 ± 2.79%), whereas peanut flower performed better in the Fru-BSA model. The inhibition rates at 0.1 g/mL (−15.20 ± 1.43%) and 0.01 g/mL (−1.49 ± 0.45%) of peanut flower in the Glu-BSA model were both negative, suggesting that lower concentrations of peanut flowers may stimulate the formation of AGEs. Similar results were obtained by Gao et al., where chamomile extract exhibited certain antiglycative effects across various concentration gradients in the Fru-BSA model and at the 2 g/mL concentration in the Glu-BSA model. However, at 0.2 g/mL and 0.02 g/mL dilutions in Glu-BSA model, the inhibition rate of AGEs was negative (Jiayang Gao et al., 2020). This implies that the antiglycative activity of certain plants is
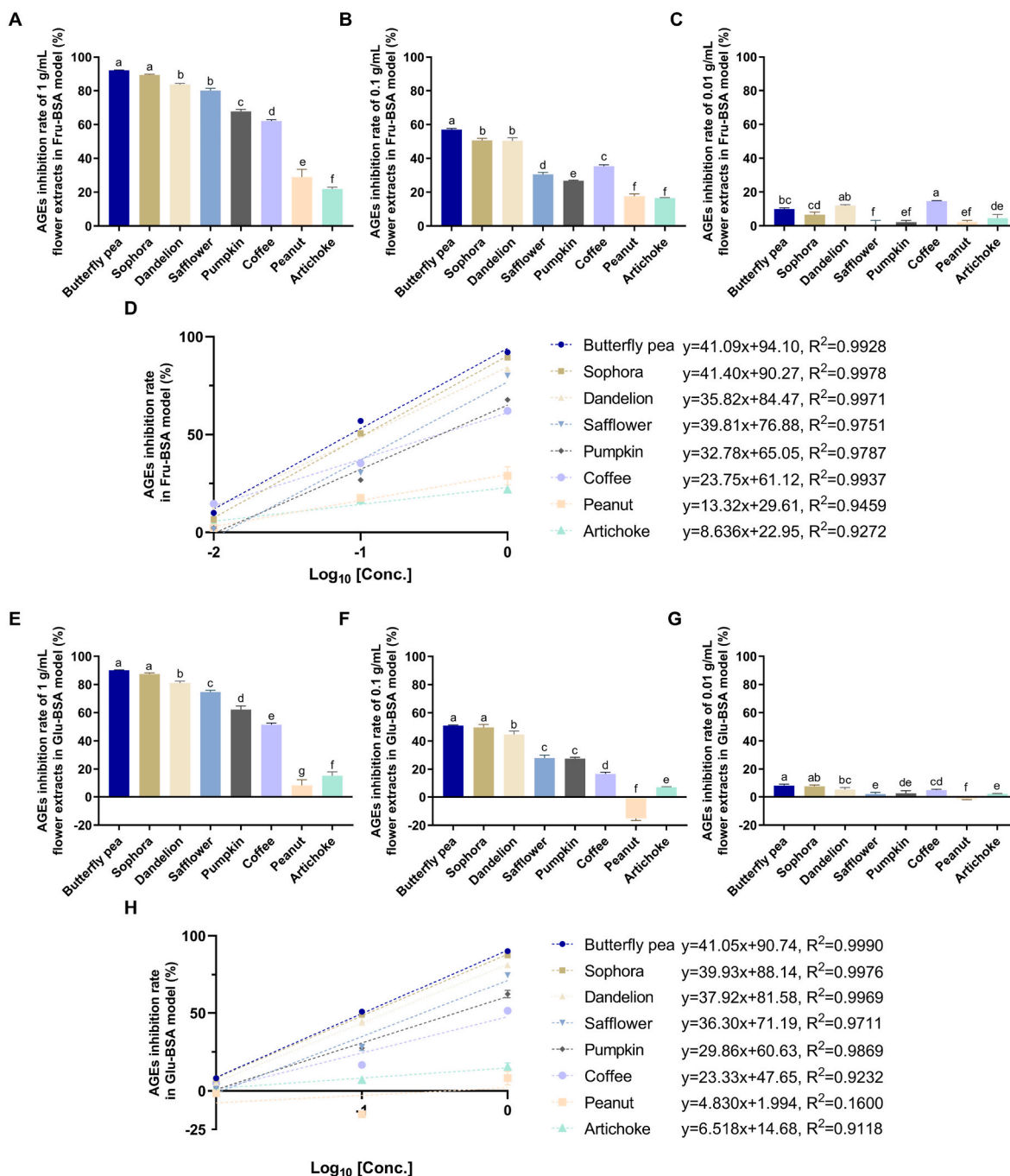
Fig. 1. The comparison of antiglycative activity of eight edible flowers in Fru-BSA model (A–D) and Glu-BSA model (E–H). AGEs inhibition rate of 1 g/mL (A), 0.1 g/mL (B), 0.01 g/mL (C) flower extracts in Fru-BSA model. AGEs inhibition rate of 1 g/mL (E), 0.1 g/mL (F), and 0.01 g/mL (G) flower extracts in Glu-BSA model. (D) and (H): Linear regression analysis between the inhibition rate and the logarithm of concentration in Fru-BSA (D) and Glu-BSA (H) model. Different characters in the columns indicate significant difference ($p < 0.05$).

concentration-dependent. Therefore, a linear regression analysis of AGEs inhibition rate and logarithm of extracts concentration was performed to understand their associations (Fig. 1D and H). It was observed that the slopes for the eight flowers in Fru-BSA model were consistently positive, with R^2 values exceeding 0.9. This signified a positive correlation between the AGEs inhibition rate and the concentration of flowers. However, the $R^2 = 0.1600$ for peanut flower in the Glu-BSA model possibly indicated an independent relationship between its concentration and AGEs inhibition rate. Furthermore, the data reveals that BFPF possessed the highest slope in both model systems, indicating its strong antiglycative ability at low concentrations. And increasing the

concentration of BFPF can substantially improve its antiglycative effect (Rodríguez-Barranco et al., 2017). Collectively, our findings highlighted the robust antiglycative activity of BFPF in both models and it was chosen for the following experiments.

3.2. Fractionation and identification of the active components in butterfly pea flower

Solvents of different polarity, including petroleum ether, n-hexane, ethyl acetate, 95% ethanol, and distilled water, were used to extract BFPF. Following that, open-column chromatography of silica gel

(200–300 mesh) and Sephadex LH-20 was performed to fractionate functional substances. Notably, the antiglycative effect of 95% ethanol (31.04 ± 1.11%) and water extracts (34.46 ± 0.95%) surpassed that of the other three solvents (Fig. 2A). Subsequently, the two extracts were combined for the first silica gel column separation, yielding 16 fractions. A1-A5 exhibited a light green color, A6-A8 displayed a light-yellow color, and A9-A26 had a dark to light blue color. The antiglycative activity of these fractions is depicted in Fig. 2B, revealing a significant AGEs inhibitory effect of fraction A9. A second round of silica gel column separation was conducted. The efficacious fractions were selected, combined, rotary evaporated, and loaded onto a Sephadex LH-20 column for further separation. A total of 13 fractions were finally obtained through methanol elution, and subsequent antiglycative tests led to the isolation of relatively pure fraction C7 for further chromatographic analyses.

By combining the chromatographic data in Figs. 2–3 and also with reference to previously published data (Escher et al., 2020; Kazuma et al., 2003a, 2003b; Nair et al., 2015; Yu et al., 2023), four compounds were preliminarily identified in fraction C7 (Fig. 3F–N). They were identified as QCT-Rh (compound 1), KFR-Rh (compound 2), rutin (compound 3), and KFR-Ne (compound 4). Intriguingly, all of the identified compounds were flavonol glycosides, with the aglycone being either kaempferol or quercetin. This might be because BFP is a dicotyledonous plant and flavonol glycosides are widely distributed in dicotyledonous plants, particularly in their floral and foliar tissues (Jinming Gao, 2017). Moreover, all glycosides were found to be attached at the C3 position of the aglycone. In plants, flavonoid glycosides typically occur at -C3 or -C7 positions (Kumar and Pandey, 2013; Mander and Liu, 2010; Zhou et al., 2020), which may be associated with the expression of uridine diphosphate-sugar-dependent glycosyltransferases (UGTs). As supported, Liu et al. isolated highly expressed UGTs in sweet orange fruits, demonstrating that various flavonoid substrates, including quercetin and kaempferol, were glycosylated at their 3- and/or 7-hydrogen

sites by these enzymes (Liu et al., 2018).

3.3. Kaempferol glycosides act as the main antiglycative compounds in butterfly pea flower

The content of the four compounds in BFPF was quantified. All standards were prepared in a concentration range from 0 to 1 mM. Their standard curves were QCT-Rh: $y = 10846x - 100149$, $R^2 = 0.9964$; KFR-Rh: $y = 7726.2x - 286560$, $R^2 = 0.9883$; rutin: $y = 13801x + 235126$, $R^2 = 0.9974$; and KFR-Ne: $y = 9187.5x - 79817$, $R^2 = 0.9919$. The limit of detection (LOD) and limit of quantification (LOQ) were as follows: 2.81 nM and 8.51 nM for QCT-Rh, 15.84 nM and 48.01 nM for KFR-Rh, 4.07 nM and 12.34 nM for rutin, 3.12 nM and 9.46 nM for KFR-Ne. The concentration of the four compounds was 97.20 mg/kg, 764.31 mg/kg, 45.56 mg/kg, and 1135.10 mg/kg, respectively, indicating a significantly higher content of kaempferol glycosides than quercetin glycosides. The AGEs-inhibitory effect of these two kaempferol glycosides was further assessed in the Fru-BSA model (Fig. 4A), indicating that the efficiency of KFR-Ne surpassed that of KFR-Rh. Hence, our data implied that the antiglycative effect of BFPF was mainly attributed to kaempferol glycosides. The IC$_{50}$ of their AGEs inhibitory rate was determined as KFR-Ne at 131.03 ± 0.75 μM and KFR-Rh at 182.17 ± 2.36 μM, with their aglycone KFR at 71.26 ± 0.44 μM (Fig. 4B). Intriguingly, the antiglycative effect of KFR decreased with the addition of glycosides, and the effect decreased with the increment in the number of glycosides (two for KFR-Rh and one for KFR-Ne). This is in line with our previous findings (Zhou et al., 2020). Given the studies of antiglycation were mostly focused on flavonoid aglycones (e.g., kaempferol and quercetin) (Bangar et al., 2023; Lai and Wong, 2022), it is crucial to address that these flavonoids are commonly present in the form of glycosides in plants (Williamson et al., 2018). For instance, glycosides of kaempferol and quercetin have been identified in the fruit of apple rather than kaempferol and quercetin themselves (Fang et al., 2022). Consequently,
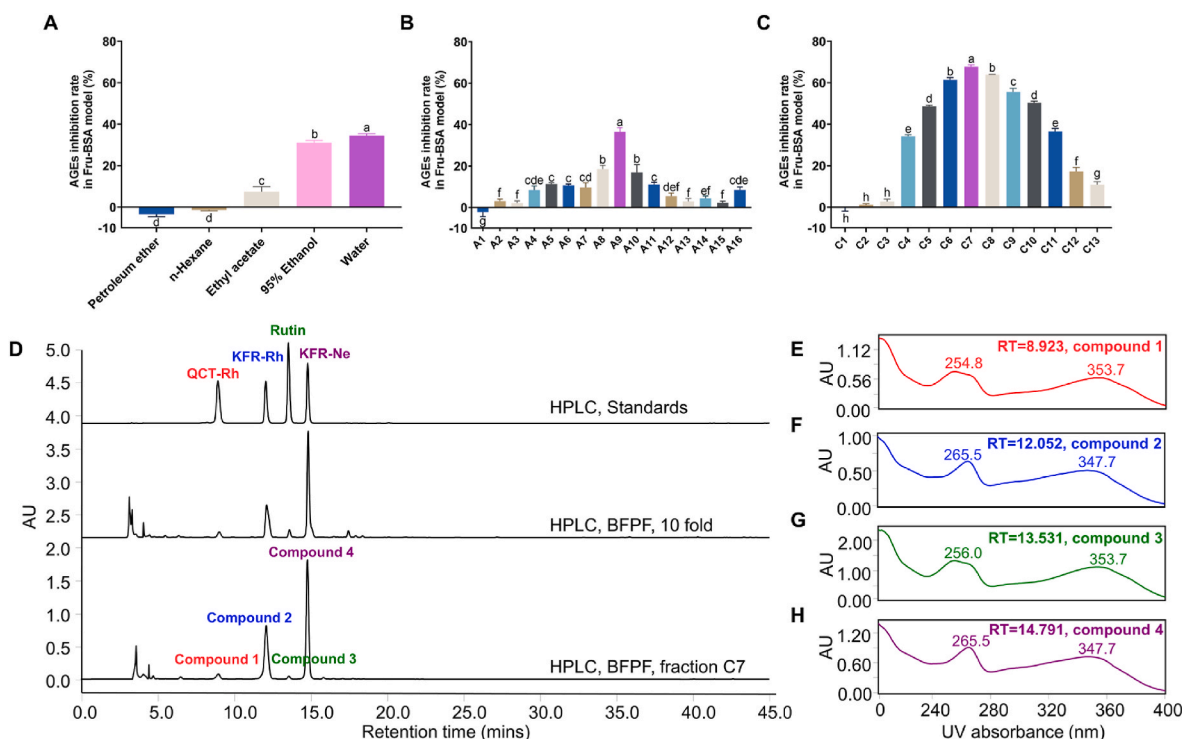

Fig. 2. Fractionation and identification of the active compounds in BFPF via HPLC analysis. (A) Solvent extraction (petroleum ether, n-hexane, ethyl acetate, 95% ethanol, and water). (B) Silica gel column fractionation of combined water and 95% ethanol extracts. (C) Sephadex LH-20 column fractionation of A9 elute. (D) HPLC chromatograms of 95% EtOH extract (0.1 g/mL), fraction C7, and four standard compounds (1 mM). Compound 1: quercetin 3-2″-rhamnosylrutinoside (QCT-Rh), compound 2: kaempferol 3–2″-rhamnosylrutinoside (KFR-Rh), compound 3: quercetin 3-rutinoside (rutin), and compound 4: kaempferol 3-neohesperidoside (KFR-Ne). (E–H) UV absorbances of compound 1–4. The detective wavelength is 265.5 nm. Different characters in the columns indicate significant difference ($p < 0.05$).
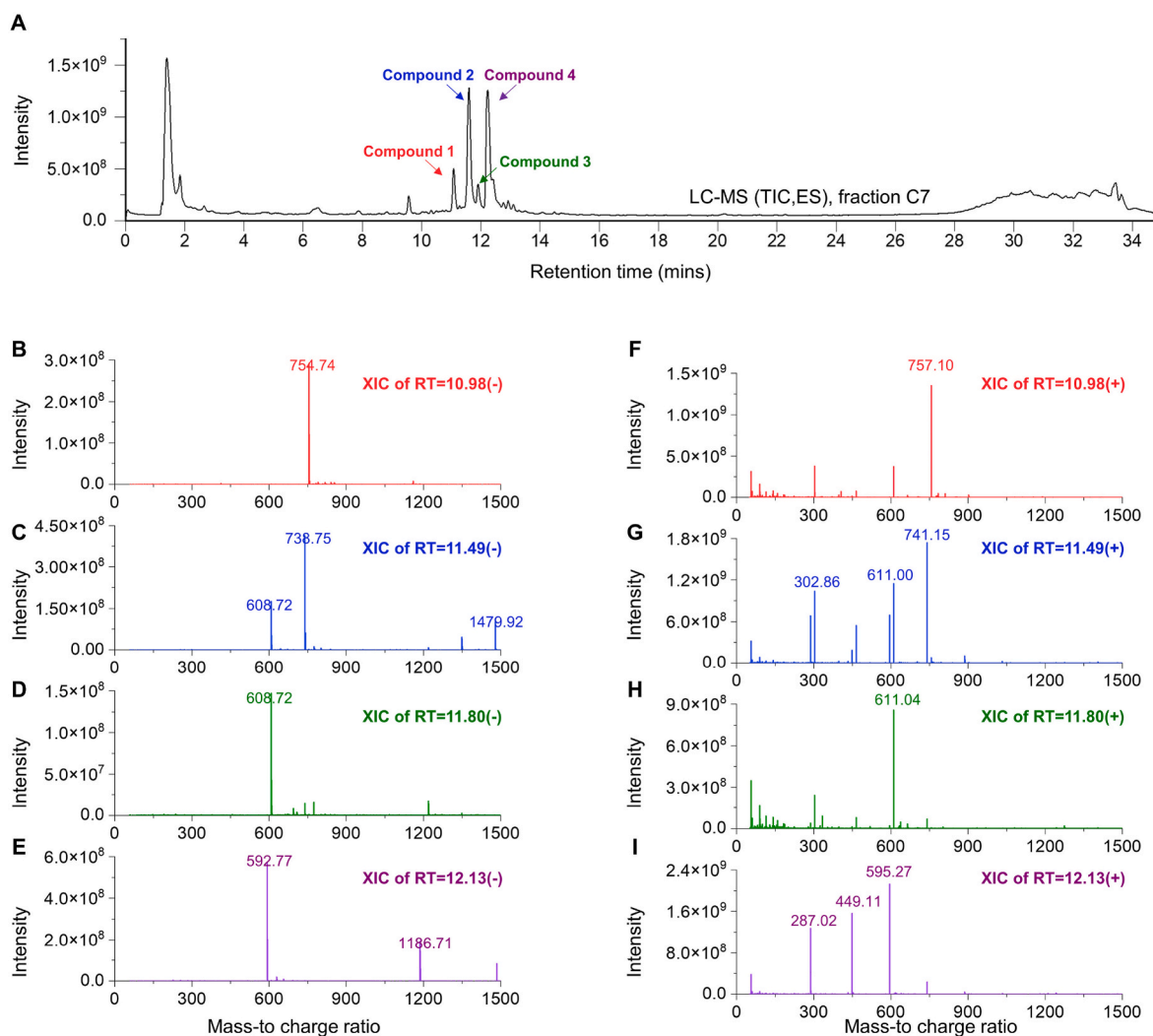
Fig. 3. Characterization of active components in BFPF via LC-MS analysis. (A) TIC of C7 fraction in negative mode. (B–E) XICs (−) of Compound 1–4. (F–I) XICs (+) of Compound 1–4.

the identification of compounds with genuine antiglycative properties in plants and diets is essential. Moreover, it is better to directly derive health benefits from daily diets rather than relying on specialized chemicals or drugs. Considering that BFPF has been commonly employed in beverages and bakery foods, the present study might probably promote more dietary application of BFPF by confirming its antiglycative effect and identifying its active compounds. Additionally, it is noteworthy that Chayaratanasin et al. conducted a preliminary antiglycative evaluation of BFPF in the Year 2015, without identifying the specific antiglycative compounds (Chayaratanasin et al., 2015). However, the present study established a detailed analysis of the antiglycative properties of BFPF and its particular active components.

3.4. Unraveling the antiglycative mechanism of kaempferol glycosides via molecular docking and NMR analysis

MD serves as a vital analytical tool to evaluate the interactions between molecules, such as proteins and polyphenols (Satish et al., 2017). In this study, Autodock 4.2.6 software and AutoDockTools 1.5.6 were employed to elucidate the binding patterns between kaempferol glycosides and BSA. The interactions of Fru-BSA and KFR-BSA were also conducted as reference data. Blind docking was initially conducted due to the undefined active center of BSA. Our results showed that the docking between fructose and BSA revealed relatively higher binding

energies (−1.77 kcal/mol), indicating a sluggish reaction between BSA and fructose. Following that, docking experiments involving KFR, KFR-Rh, and KFR-Ne with BSA were performed (−5.33 kcal/mol, −3.13 kcal/mol, −2.55 kcal/mol) and demonstrated a superior binding capability compared to fructose and BSA. To further elucidate the active sites of BSA, an online resource called Proteins. plus (https://proteins.plus/, using DoGSiteScorer module) was employed to predict the most possible binding sites. As a result, a pocket with 1108.42 Å^3 volume, 1304.18 Å^2 surface in chain A of 4f5s got the highest score and was used (pocket containing residue 194, 197, 198, 201, 205, 208 to 213, 215, 217, 227, 230, 231, 234, 323, 324, 326, 327, 330, 342, 343, 346, 347, 349, 350, 353, 449, 450, 452 to 454, 456, 457, and 479 to 485). Subsequently, KFR, KFR-Rh, and KFR-Ne underwent precise docking with BSA in the predicted pocket. KFR (−6.74 kcal/mol) exhibited significant interaction with BSA, followed by KFR-Ne (−4.15 kcal/mol) and KFR-Rh (−2.87 kcal/mol), aligning with the trends on the inhibition rate of AGEs in the model system (Fig. 4A–B). As reported by Tang et al., hydroxylation at positions C3, C6, C4', and C5' was found to favor the formation of hydrogen bonds with BSA amino acids, whilst glycosylation at C3 and C7 may reduce their affinity (Tang et al., 2020). Therefore, KFR glycosylation may hinder BSA binding to its active hydroxyl group. Further analyses using PyMOL 2.2.0 (Schrödinger Inc., NY, USA) revealed that the three flavonoids formed hydrophobic interactions and hydrogen bonding interactions with BSA. Specifically, KFR formed
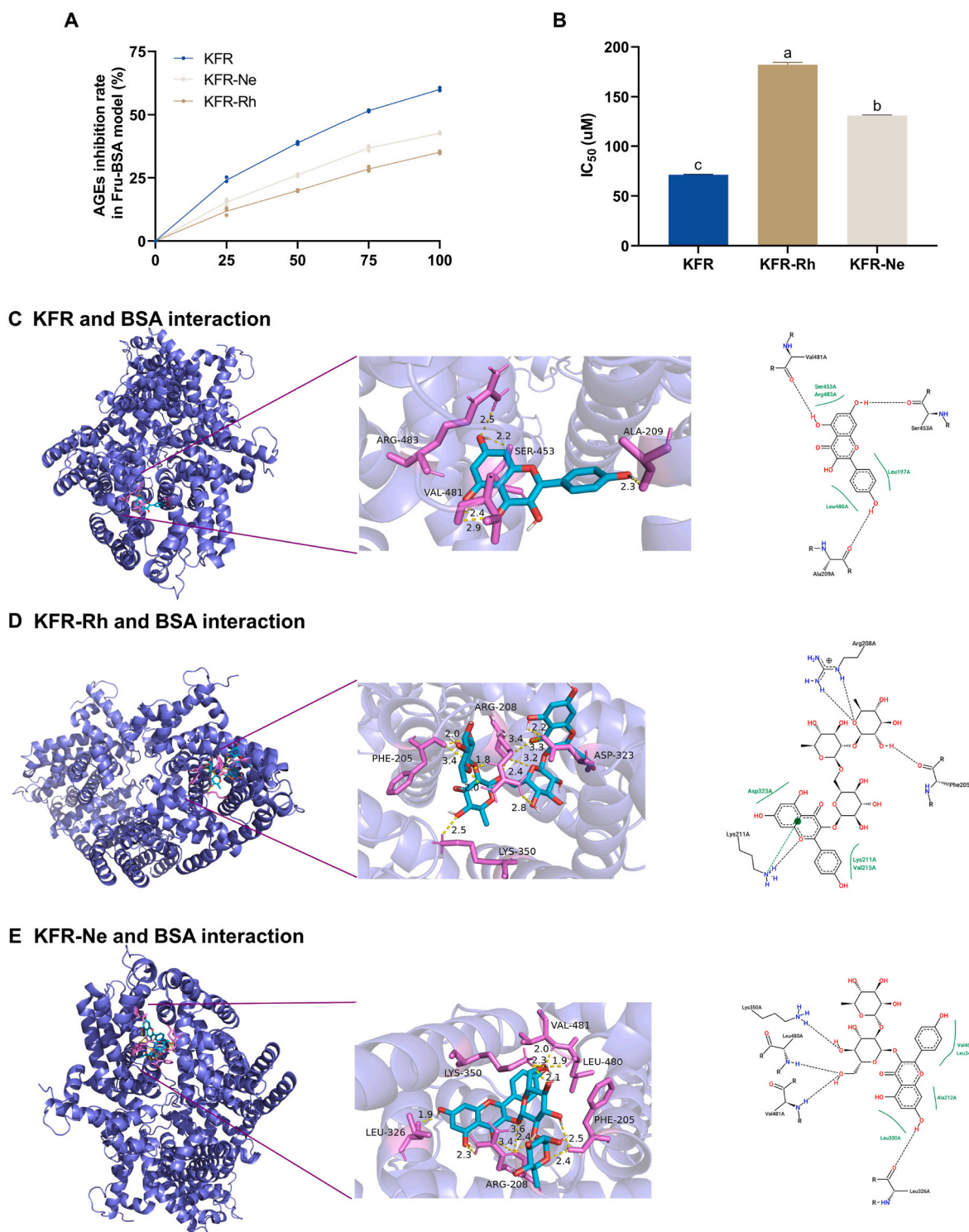
Fig. 4. (A) AGEs inhibition rate of KFR, KFR-Rh, and KFR-Ne in Fru-BSA model. (B) IC$_{50}$ of three standards in Fru-BSA model. (C–E) Molecular docking of the standards with BSA. In 3D figures, ligands are shown in cyanine blue color, interacted residues of BSA are shown in purplish red color, and hydrogen bonds are shown in yellow color. In 2D figures, hydrogen bonds are presented in black dashed lines, and hydrophobic contact is presented in green lines. Different characters in the columns indicate significant difference ($p < 0.05$). (For interpretation of the references to color in this figure legend, the reader is referred to the Web version of this article.)

hydrogen bonding interactions at the Ala 209, Ser 453, and Val 481 positions of BSA (Fig. 4C). Moreover, hydrophobic interaction in KFR-BSA existed in Ser 453, Arg 483, Leu 197, and Leu 480. Our findings were in line with Me et al., who demonstrated that hydrogen bonding may serve as a non-covalent bond in the binding of BSA with KFR (Ma et al., 2023). Similarly, KFR-Ne and KFR-Rh interacted with BSA

through hydrogen bonding and hydrophobic interactions, but weaker than KFR. In detail, KFR-Rh formed hydrogen binding interactions at Arg 208, Lys 211, and Phe 205 (Fig. 4D), while KFR-Ne was at Lys 350, Leu 480, Val 481, and Leu 326 (Fig. 4E). Noteworthy, the rutinose in KFR-Rh and the neohesperidoside in KFR-Ne can also form hydrogen bonding interactions with BSA (Fig. 4D–E). This is supported by Bi et al.

that Trp 213,Tyr 155, Lys 211, Ala 212 of rutinose on eriodictioside were found to interact with BSA (Bi et al., 2020). For the hydrophobic interactions, it occurred at Asp 323, Lys 211, Val 215 in KFR-Rh and at Val 481, Leu 346, Ala 212, Leu 330 in KFR-Ne.

NMR spectroscopy provides a non-destructive and non-disruptive evaluation of chemical binding reactions, making it a popular method in the study of polyphenol-protein interactions. As illustrated in Fig. 5, the chemical shifts were observed at the molar ratio of 100:1 (Fig. 5A–B). Compared to KFR-Ne (Fig. 5A, blue line), after a 7-day incubation of KFR-Ne with BSA (Fig. 5A, orange line), the proton signals broadened and some sharp peaks merged, indicating an interaction between BSA and KFR-Ne. For instance, the chemical shifts of H6 and H8, H2′, H3′, H5′, and H6' on the diphenylchromone core of KFR-Ne

moved upfield, suggesting a π-π interaction between these aromatic carbons and the aromatic amino acids of BSA (X. Peng et al., 2015). Notably, the upfield shifts of H8 and H6 were more pronounced. Additionally, protons on the glycoside exhibited slight downfield shifts and peak merging, implying potential interactions between them and BSA (Chuan ying et al., 2021). Given that the primary hydrophobic groups on KFR-Ne are the two benzene rings which play a crucial role in the interaction, we inferred that there was a hydrophobic force between BSA and KFR-Ne. This is in consistent with the findings by Zhang et al., who observed upfield shifts of benzene ring hydrogens in salvianolic acid B upon interaction with BSA (Chuan ying et al., 2021). Moreover, chlorogenic acid and neochlorogenic acid in chrysanthemum flower showed hydrophobic interaction with BSA (Wang et al., 2024).
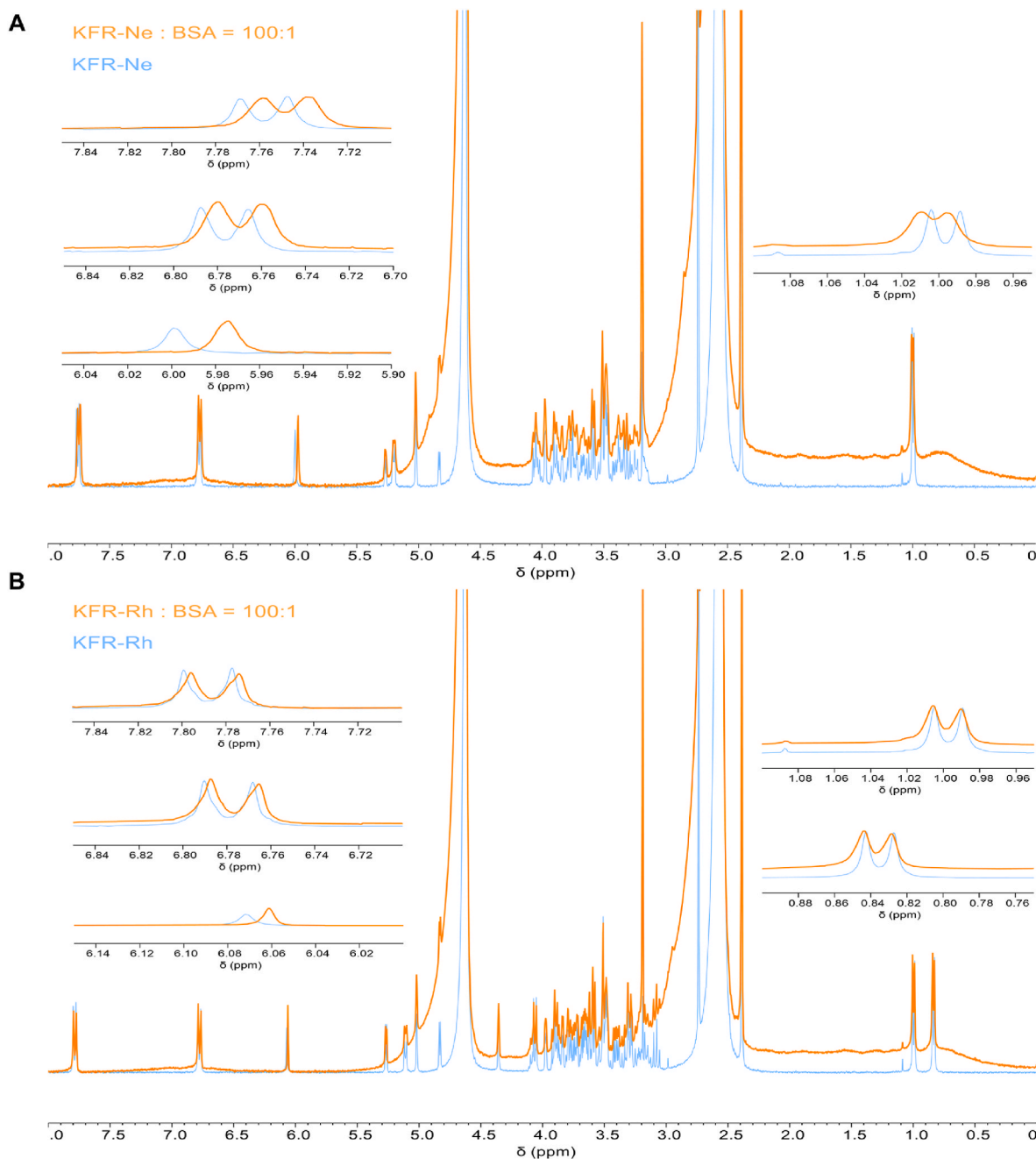

Fig. 5. ^{1}H NMR analysis of KFR-Ne, KFR-Rh, KFR-Ne-BSA and KFR-Rh-BSA. The concentration of KFR glycosides is 2.5 mM in all samples. (A) ^{1}H NMR spectra of KFR-Ne and BSA at the ratio of 100:1 (in orange), and KFR-Ne (in blue). (B) ^{1}H NMR spectra of KFR-Rh and BSA at the ratio of 100:1 (in orange), and KFR-Rh (in blue). The δ range of the enlarged graphs in C and D are all 0.15 ppm. (For interpretation of the references to color in this figure legend, the reader is referred to the Web version of this article.)

Comparing Fig. 5A–B, KFR-Rh exhibited similar chemical shift trends as KFR-Ne when interacting with BSA, but had a smaller overall deviation. This indicated a weaker interaction. These observations aligned with our MD results (Fig. 4D–E) and the inhibitory rate of AGEs in the model system (Fig. 4A–B). Collectively, our data suggest the remarkable antiglycative effect of BFPF. Such effect is attributed to the presence of KFR glycosides which can bind to BSA, occupying the active sites and thereby obstructing the sugar-protein reaction that led to glycation.

4. Conclusions

The present study used *in vitro* model to evaluate antiglycative activities of eight edible flowers. Most of them exerted appreciable antiglycative activity in model systems, except peanut flower which promoted the formation of AGEs in Glu-BSA model. Noteworthy, BFPF showed the highest AGEs inhibitory rate, with further fractionation analyses identifying the existence of QCT-Rh, KFR-Rh, rutin, and KFR-Ne in BFPF. Moreover, with reference to their content in BFPF and the IC$_{50}$ of their AGEs inhibitory rate, KFR-Ne and KFR-Rh were indicated as the major antiglycative components in BFPF. Finally, both KFR-Ne and KFR-Rh showed hydrophobic and hydrogen bonding interactions with BSA on the flavonoid aglycone and the sugar moiety. To the best of our knowledge, it is the first report to establish the specific antiglycative compounds in BFPF by far. In summary, the present study revealed the antiglycative effect of BFPF and identified its active phytochemicals. Our findings are useful for the development of BFPF-based products with functional applications. This is particularly relevant considering the growing demand for anti-aging practices in recent years.

CRediT authorship contribution statement

Jun Wu: Conceptualization, Methodology, Investigation, Formal analysis, Data curation, Writing – original draft, Visualization. **Jun Gong:** Formal analysis, Visualization. **Qiaochun Chen:** Methodology, Formal analysis. **Wen Hao:** Investigation, Writing – review & editing. **Jiayi He:** Methodology, Writing – review & editing. **Mingfu Wang:** Conceptualization, Writing – review & editing, Supervision, Project administration, Funding acquisition. **Qian Zhou:** Conceptualization, Methodology, Writing – original draft, Writing – review & editing, Funding acquisition, Project administration.

Declaration of competing interest

The authors declare that they have no known competing financial interests or personal relationships that could have appeared to influence the work reported in this paper.

Acknowledgments

Data availability

Data will be made available on request.

References

Bangar, S.P., Chaudhary, V., Sharma, N., Bansal, V., Ozogul, F., Lorenzo, J.M., 2023. Kaempferol: a flavonoid with wider biological activities and its applications. Crit. Rev. Food Sci. Nutr. 63 (28), 9580–9604. https://doi.org/10.1080/10408398.2022.2067121.

Bi, S., Wu, J., Sun, X., Zhao, R., Shao, D., Li, X., 2020. Spectral and molecular docking studies on the interaction of three flavonoids with bovine serum albumin. J. Biomol. Struct. Dyn. 38 (7), 2197–2205. https://doi.org/10.1080/07391102.2019.1624196.

Chaudhuri, J., Bains, Y., Guha, S., Kahn, A., Hall, D., Bose, N., Gugliucci, A., Kapahi, P., 2018. The role of advanced glycation end products in aging and metabolic diseases: bridging association and causality. Cell Metabol. 28 (3), 337–352, 10.1016%2Fj.cmet.2018.08.014.

Chayaratanasin, P., Barbieri, M.A., Suanpairintr, N., Adisakwattana, S., 2015. Inhibitory effect of Clitoria ternatea flower petal extract on fructose-induced protein glycation and oxidation-dependent damages to albumin in vitro. BMC Compl. Alternative Med. 15, 1–9. https://doi.org/10.1186/s12906-015-0546-2.

Chen, Q., Xu, B., Huang, W., Amrouche, A.T., Maurizio, B., Simal-Gandara, J., Tundis, R., Xiao, J., Zou, L., Lu, B., 2020. Edible flowers as functional raw materials: a review on anti-aging properties. Trends Food Sci. Technol. 106, 30–47. https://doi.org/10.1016/j.tifs.2020.09.023.

Chuan ying, Z., Xin, P., Heng jun, R., Wei, Q., Rong-xin, S., Zhi-min, H., 2021. Spectroscopic studies on the interaction between salvianolic acid B and bovine serum albumin. Spectrosc. Spectr. Anal. 41 (6), 1701–1707. https://doi.org/10.3964/j.issn.1000-0593(2021)06-1701-07.

Escher, G.B., Wen, M., Zhang, L., Rosso, N.D., Granato, D., 2020. Phenolic composition by UHPLC-Q-TOF-MS/MS and stability of anthocyanins from Clitoria ternatea L. (butterfly pea) blue petals. Food Chem. 331, 127341. https://doi.org/10.1016/j.foodchem.2020.127341.

Fang, T., Chen, J., Lin, Q., Zhong, Y., Duan, Y., Bi, J., 2022. Phenolic profiling reveals the metabolite basis of flesh colour and fresh-cut browning in apple fruit. Int. J. Food Sci. Technol. 57 (4), 2257–2266. https://doi.org/10.1111/ijfs.15575.

Gao, J., 2017. Phytochemical, third ed. China Science Publishing and Media Ltd, Beijing, China.

Gao, J., Sun, Y., Li, L., Zhou, Q., Wang, M., 2020. The antiglycative effect of apple flowers in fructose/glucose-BSA models and cookies. Food Chem. 330, 127170. https://doi.org/10.1016/j.foodchem.2020.127170.

Gugliucci, A., 2017. Formation of fructose-mediated advanced glycation end products and their roles in metabolic and inflammatory diseases. Adv. Nutr. 8 (1), 54–62. https://doi.org/10.3945/an.116.013912.

Hashim, S.B., Tahir, H.E., Liu, L., Zhang, J., Zhai, X., Mahdi, A.A., Awad, F.N., Hassan, M. M., Xiaobo, Z., Jiyong, S., 2022. Intelligent colorimetric pH sensoring packaging films based on sugarcane wax/agar integrated with butterfly pea flower extract for optical tracking of shrimp freshness. Food Chem. 373, 131514. https://doi.org/10.1016/j.foodchem.2021.131514.

Jaglanian, A., Termini, D., Tsiani, E., 2020. Rosemary (Rosmarinus officinalis L.) extract inhibits prostate cancer cell proliferation and survival by targeting Akt and mTOR. Biomed. Pharmacother. 131, 110717. https://doi.org/10.1016/j.biopha.2020.110717.

Jeyaraj, E.J., Lim, Y.Y., Choo, W.S., 2021. Extraction methods of butterfly pea (Clitoria ternatea) flower and biological activities of its phytochemicals. J. Food Sci. Technol. 58 (6), 2054–2067, 10.1007%2Fs13197-020-04745-3.

Kazuma, K., Noda, N., Suzuki, M., 2003a. Flavonoid composition related to petal color in different lines of Clitoria ternatea. Phytochemistry 64 (6), 1133–1139. https://doi.org/10.1016/s0031-9422(03)00504-1.

Kazuma, K., Noda, N., Suzuki, M., 2003b. Malonylated flavonol glycosides from the petals of Clitoria ternatea. Phytochemistry 62 (2), 229–237. https://doi.org/10.1016/S0031-9422(02)00486-7.

Kumar, S., Pandey, A.K., 2013. Chemistry and biological activities of flavonoids: an overview. Sci. World J. 2013. https://doi.org/10.1155/2013/162750.

Lai, W.F., Wong, W.T., 2022. Design and optimization of quercetin-based functional foods. Crit. Rev. Food Sci. Nutr. 62 (26), 7319–7335. https://doi.org/10.1080/10408398.2021.1913569.

Li, X.H., He, X.R., Zhou, Y.Y., Zhao, H.Y., Zheng, W.X., Jiang, S.T., Zhou, Q., Li, P.P., Han, S.Y., 2017. Taraxacum mongolicum extract induced endoplasmic reticulum stress associated-apoptosis in triple-negative breast cancer cells. J. Ethnopharmacol. 206, 55–64. https://doi.org/10.1016/j.jep.2017.04.025.

Liu, X., Lin, C., Ma, X., Tan, Y., Wang, J., Zeng, M., 2018. Functional characterization of a flavonoid glycosyltransferase in sweet orange (Citrus sinensis). Front. Plant Sci. 9, 317010. https://doi.org/10.3389/fpls.2018.00166.

López Prado, A.S., Shen, Y., Ardoin, R., Osorio, L.F., Cardona, J., Xu, Z., Prinyawiwatkul, W., 2019. Effects of different solvents on total phenolic and total anthocyanin contents of Clitoria ternatea L. petal and their anti-cholesterol oxidation capabilities. Int. J. Food Sci. Technol. 54 (2), 424–431. https://doi.org/10.1111/ijfs.13953.

Ma, R.H., Wang, W., Hou, C.-P., Man, Y.F., Ni, Z.J., Thakur, K., Zhang, J.G., Wei, Z.J., 2023. Structural characterization and stability of glycated bovine serum albumin-kaempferol nanocomplexes. Food Chem. 415, 135778. https://doi.org/10.1016/j.foodchem.2023.135778.

Mander, L., Liu, H.W., 2010. Comprehensive Natural Products II: Chemistry and Biology, vol. 1. Elsevier Science, Amsterdam, Netherlands.

Nair, V., Bang, W.Y., Schreckinger, E., Andarwulan, N., Cisneros Zevallos, L., 2015. Protective role of ternatin anthocyanins and quercetin glycosides from butterfly pea (Clitoria ternatea Leguminosae) blue flower petals against lipopolysaccharide (LPS)-induced inflammation in macrophage cells. J. Agric. Food Chem. 63 (28), 6355–6365. https://doi.org/10.1021/acs.jafc.5b00928.

Peng, H., Gao, Y., Zeng, C., Hua, R., Guo, Y., Wang, Y., Wang, Z., 2024. Effects of Maillard reaction and its product AGEs on aging and age-related diseases. Food Sci. Hum. Wellness 13 (3), 1118–1134. https://doi.org/10.26599/FSHW.2022.9250094.

Peng, X., Wang, X., Qi, W., Huang, R., Su, R., He, Z., 2015. Deciphering the binding patterns and conformation changes upon the bovine serum albumin–rosmarinic acid complex. Food Funct. 6 (8), 2712–2726. https://doi.org/10.1039/C5FO00597C.

Rivas García, L., Navarro Hortal, M.D., Romero Márquez, J.M., Forbes Hernández, T.Y., Varela López, A., Llopis, J., Sánchez González, C., Quiles, J.L., 2021. Edible flowers

as a health promoter: an evidence-based review. Trends Food Sci. Technol. 117, 46–59. https://doi.org/10.1016/j.tifs.2020.12.007.

Rodríguez-Barranco, M., Tobías, A., Redondo, D., Molina-Portillo, E., Sánchez, M.J., 2017. Standardizing effect size from linear regression models with log-transformed variables for meta-analysis. BMC Med. Res. Methodol. 17, 1–9. https://doi.org/10.1186/s12874-017-0322-8.

Satish, L., Millan, S., Bera, K., Mohapatra, S., Sahoo, H., 2017. A spectroscopic and molecular dynamics simulation approach towards the stabilizing effect of ammonium-based ionic liquids on bovine serum albumin. New J. Chem. 41 (19), 10712–10722. https://doi.org/10.1039/C7NJ02900D.

Shen, Y., Du, L., Zeng, H., Zhang, X., Prinyawiwatkul, W., Alonso Marenco, J.R., Xu, Z., 2016. Butterfly pea (Clitoria ternatea) seed and petal extracts decreased HE p-2 carcinoma cell viability. Int. J. Food Sci. Technol. 51 (8), 1860–1868. https://doi.org/10.1111/ijfs.13158.

Tang, H., Huang, L., Zhao, D., Sun, C., Song, P., 2020. Interaction mechanism of flavonoids on bovine serum albumin: insights from molecular property-binding affinity relationship. Spectrochim. Acta Mol. Biomol. Spectrosc. 239, 118519. https://doi.org/10.1016/j.saa.2020.118519.

Wang, Z., Zhu, Y., Xu, M., Peng, K., Shi, B., Wang, Y., Chen, Q., Huang, W., Chen, Y., Lu, B., 2024. Chrysanthemum as a remarkable edible flower resource with anti-glycation effects: representative variety differences, phenolic compositions, and the interaction mechanism. Food Frontiers 5 (3), 907–919. https://doi.org/10.1002/fft2.385.

Wen, Y., Liu, Y., Huang, Q., Farag, M.A., Li, X., Wan, X., Zhao, C., 2022. Nutritional assessment models for diabetes and aging. Food Frontiers 3 (4), 689–705. https://doi.org/10.1002/fft2.168.

Williamson, G., Kay, C.D., Crozier, A., 2018. The bioavailability, transport, and bioactivity of dietary flavonoids: a review from a historical perspective. Compr. Rev. Food Sci. Food Saf. 17 (5), 1054–1112. https://doi.org/10.1111/1541-4337.12351.

Yu, Q., Yu, F., Li, Q., Zhang, J., Peng, Y., Wang, X., Li, T., Yin, N., Sun, G., Ouyang, H., 2023. Anthocyanin-rich butterfly pea flower extract ameliorating low-grade inflammation in a high-fat-diet and lipopolysaccharide-induced mouse model. J. Agric. Food Chem. 71 (31), 11941–11956. https://doi.org/10.1021/acs.jafc.3c02696.

Yue, K., Mao, B., Tang, X., Zhang, Q., Zhao, J., Cui, S., Chen, W., 2023. Recent updates in anti-glycation strategies: selection of natural products and lactic acid bacteria as potential inhibitors based on the multi-pathway anti-glycation targets. Crit. Rev. Food Sci. Nutr. 1–18. https://doi.org/10.1080/10408398.2023.2232015.

Zhou, Q., Cheng, K.W., Xiao, J., Wang, M., 2020. The multifunctional roles of flavonoids against the formation of advanced glycation end products (AGEs) and AGEs-induced harmful effects. Trends Food Sci. Technol. 103, 333–347. https://doi.org/10.1016/j.tifs.2020.06.002.

Zhou, Q., Wang, L., Liu, B., Xiao, J., Cheng, K.W., Chen, F., Wang, M., 2021. Tricoumaroylspermidine from rose exhibits inhibitory activity against ethanol-induced apoptosis in HepG2 cells. Food Funct. 12 (13), 5892–5902. https://doi.org/10.1039/D1FO00800E.